separations

MDPI

Article

Enhancement of the Wastewater Treatment Process of a PETRO System by Natural and Commercial Coagulants

Phillimon Tlamelo Odirile [1,*] and Nkgopolang Matthews Boima [1,2]

[1] Department of Civil Engineering, Faculty of Engineering & Technology, University of Botswana, Gaborone Private Bag UB 0022, Botswana; nboima@wuc.bw
[2] Water Utilities Corporation, Gaborone Private Bag 00276, Botswana
* Correspondence: odirilep@ub.ac.bw

Abstract

Water pollution due to insufficient wastewater treatment is a global concern. In this paper, coagulation and flocculation as a tertiary polishing unit process were investigated to find a solution for a non-compliant wastewater treatment facility. The Palapye Pond Enhanced Treatment and Operation (PETRO) system has not been compliant for a long time with effluent characterised by high turbidity, Biological Oxygen Demand/Chemical Oxygen Demand (BOD/COD), Total Suspended Solids (TSS), Nitrates (NO_3^-), and Phosphates (PO_4^{3-}) The effluent from the plant is released into the stream that drains into the nearby Lotsane dam, posing significant danger to the water quality of the dam. The main objective of the study was to investigate the effect of coagulation and flocculation processes at the tertiary stage of the wastewater treatment process. Response Surface Methodology (RSM), Central Composite Design (CCD) and Multi Response Surface (MRS) were used to optimise the coagulation process and generate regression models to predict the coagulation and flocculation. The performance was evaluated using turbidity, Colour, COD and TSS as response variables. Response surface analysis indicated that the experimental data could be adequately fitted to quadratic polynomial models. Under optimum conditions the removal efficiency for $Al_2(SO_4)_3 \cdot 18H_2O$: 91.1% (turbidity), 88.2% (colour), 58.9% (COD), 83.0% (TSS); for $FeCl_3 \cdot 6H_2O$: 93.2%, 88.7%, 63.8%, 91.3%; for Moringa: 91.8%, 85.4%, 56.6%, 83.7%. The optimal removals based on MRS for $Al_2(SO_4)_3.18H_2O$, $FeCl_3.6H_2O$ and *Moringa oleifera* were 90.7%, 89.7%, 59.9% and 88.5%; 94.7%, 90.8%, 58.1% and 93.8%; 94.0%, 87.2%, 60.1% and 82.1% for turbidity, colour, COD and TSS respectively. This research has demonstrated that the coagulation/flocculation process, operating synergistically with pH-induced precipitation softening, can be incorporated as an enhancement to the secondary treatment stage of the wastewater treatment facility. At the optimal alkaline conditions (pH 12–12.6), the dominant mechanism is the precipitation of native hardness ions (Mg^{2+}, Ca^{2+}) as $Mg(OH)_2$ and $CaCO_3$, which enmesh colloidal particles, while the added coagulants play a refining role by enhancing floc structure and settling. The study introduces a comparative evaluation of three coagulants within a single RSM-CCD optimisation framework, employing desirability functions for multi-response optimisation.

Keywords: Response Surface Methodology; central composite design; Multi Response Surface; pH-induced coagulation; flocculation; PETRO; wastewater treatment

Academic Editor: Xiaomin Ma

Received: 8 February 2026
Revised: 9 April 2026
Accepted: 20 April 2026
Published: 5 May 2026

1. Introduction

Wastewater treatment is a critical environmental intervention aimed at removing pollutants from domestic and industrial effluents to protect public health and receiving

water bodies [1]. Two predominant treatment approaches are widely employed: the activated sludge (AS) system and the pond system. The selection between these hinges on factors such as land availability and capital resources. Pond systems, while requiring larger land areas, offer lower operational costs, whereas AS systems are favoured where land is limited but demand higher capital investment [2].

Over time, both system types can fail to perform as designed. Increasing population loads, inadequate maintenance, and ageing infrastructure often result in effluent that no longer meets regulatory standards [3]. This is precisely the situation at the Palapye wastewater treatment plant in Botswana. Originally a waste stabilisation pond (WSP) system, it was upgraded in 2005 to the Pond Enhanced Treatment and Operation (PETRO) system, incorporating trickling filters (TFs) and humus tanks (HTs) to enhance solids removal [3]. Despite this upgrade, the plant has consistently failed to comply with Botswana's discharge standards [4]. The effluent, characterised by high turbidity, COD, TSS, and nutrients, is released into a stream that drains into the Lotsane Dam, a critical local water resource. Continued non-compliance poses a significant eutrophication risk and threatens the dam's water quality, with downstream consequences for ecosystems and communities that rely on it. This environmental threat provides the urgent impetus for identifying a cost-effective upgrade solution.

Coagulation-flocculation is a well-established separation process for removing suspended and colloidal particles. While traditionally applied as a primary treatment step [5], its application as a tertiary polishing stage following biological treatment is gaining traction for achieving stringent effluent limits [6,7]. The process works by destabilising particles and aggregating them into larger flocs that can be removed by sedimentation. However, its effectiveness is highly dependent on coagulant type, dosage, and pH, necessitating systematic optimisation.

The choice of coagulants is central to process performance and cost. Metal salts like aluminium sulphate (alum) and ferric chloride are the most common synthetic coagulants, each with distinct pH optima and removal mechanisms [5,8]. Ferric salts, for instance, are often effective over a broader pH range due to the formation of various hydrolysed species [9]. In parallel, there is growing interest in natural coagulants, particularly from *Moringa oleifera* seeds, as a sustainable, biodegradable, and potentially lower-cost alternative [5,10]. *Moringa oleifera* seeds contain cationic proteins that act as effective coagulants for turbidity removal [11].

The selection of the pH range (8.38–12.6) for this study was deliberate and based on the specific characteristics of the PETRO system secondary effluent. Preliminary characterisation of the trickling filter effluent revealed significant concentrations of hardness ions (Ca^{2+}, Mg^{2+}), with total hardness averaging 180–220 mg/L as $CaCO_3$. At elevated pH (>10.5), these hardness ions precipitate as $Mg(OH)_2$ and $CaCO_3$, forming voluminous flocs that can enmesh suspended particles through a sweeping mechanism—a process known as precipitation softening or lime softening. This phenomenon is well-documented in water treatment for hardness removal but is less commonly exploited in wastewater tertiary treatment.

Rather than operating at the classical optima for metal salt coagulants (pH 5.5–7.5 for alum; pH 4–11 for ferric chloride), we hypothesised that leveraging pH-induced precipitation of native hardness ions could provide a dual benefit: (1) substantial baseline removal of turbidity, colour, and TSS through sweeping flocculation, and (2) a high-pH environment where added coagulants, although not forming traditional hydroxide precipitates, could act as bridging agents to refine floc structure and enhance settling. This synergistic approach was therefore designed to maximise overall treatment efficiency while potentially reducing coagulant demand.

Several studies have compared coagulant performance, but predominantly in synthetic waters or at the primary treatment stage [11,12]. For example, Desta and Bote [13] compared ferric chloride and alum for surface water treatment, while Sánchez-Martín et al. [12,14] evaluated purified *Moringa oleifera* coagulants. However, comparative studies evaluating both synthetic and natural coagulants specifically for tertiary polishing of municipal secondary effluent, particularly within an integrated system like the PETRO process, are scarce. Furthermore, the application of modern statistical optimisation tools to this specific context is limited.

This study addresses these gaps by providing a systematic, comparative evaluation of three coagulants ($Al_2(SO_4)_3 \cdot 18H_2O$, $FeCl_3 \cdot 6H_2O$, and *Moringa oleifera* seed powder) for tertiary treatment of the PETRO system effluent. The overarching goal is to generate actionable data that can guide a cost-effective upgrade of the Palapye facility and offer a replicable methodology for similar wastewater treatment challenges globally. The specific objectives are to: (1) determine the optimal pH and dosage conditions for each coagulant using jar tests; (2) develop and validate predictive models for turbidity, colour, COD, and TSS removal using Response Surface Methodology (RSM) with Central Composite Design (CCD); (3) apply multi-response optimisation to identify compromise conditions balancing all four water quality parameters; and (4) assess the practical viability of the optimised process by evaluating its ability to achieve regulatory compliance and estimating operational costs.

Study Area

Palapye is a large village in Botswana with suburbs and is growing rapidly. Originally, Palapye served as a railway siding. It is situated in the Central District, some 271 km from the capital Gaborone along the A1 Road towards the northern side of the country. The Palapye 2011 population census was 37,000. Located 5 km to the west of the village is the Morupule coal mine and power station that supplies electricity to the whole country of Botswana. The construction to expand the power station to meet the demand of the country started in 2010, with the construction of the Morupule Power B station. The geographical location of Palapye wastewater treatment plant (PWWTP) is latitude 22°32′26.13″ S and longitude 27°10′22.65″ E (Figure 1). The treatment plant is located northeast of the village (Figure 1). The Palapye Petro system consists of 4 facultative ponds (FPs), 1 primary pond, 3 secondary ponds, and 6 oxidation ponds as a primary treatment stage. In this system, the TF and HT, which make a secondary treatment, are used. The FP 1, TFs and HTs were introduced to enhance the performance of the already existing pond system that consisted of 3 anaerobic ponds (APs), 2 FPs and 4 maturation ponds (MPs).

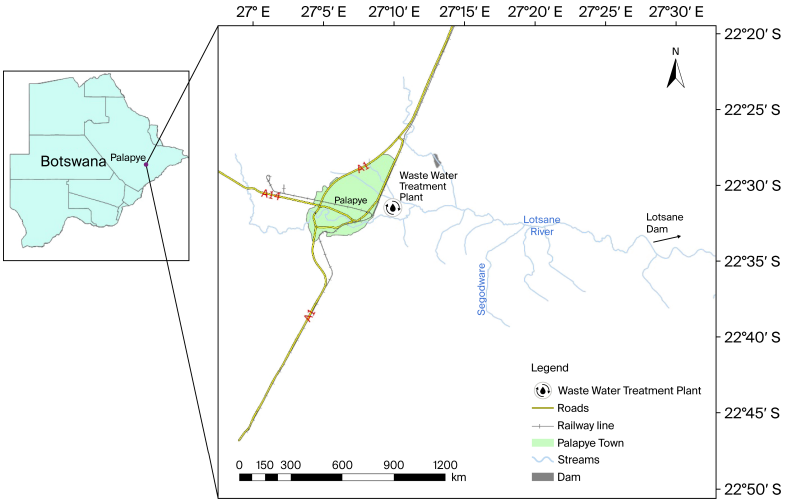

Figure 1. Location of the Palapye Wastewater Treatment Plant (PWWTP) Study Area, Botswana.

2. Materials and Methods

2.1. Sampling

The samples were collected between the TFs and the HTs, using 25-litre containers and subsequently transported to the Mmamashia laboratory for jar tests. This is the point where tertiary treatment would be introduced as shown in Figure 2. The collected TF effluent and jar test samples were meticulously preserved and analysed for turbidity, colour, COD, and TSS, in accordance with the Standard Methods for the Examination of Water and Wastewater (23rd Edition) [10]. Sampling was conducted on eight occasions between March and September 2020. Preliminary studies involved triplicate testing for each parameter. Subsequently, the 39 experimental runs required by the Response Surface Methodology (RSM) design were performed with a single test per parameter. Jar tests were conducted using a standard six-paddle jar test apparatus (Phipps & Bird, Richmond, VA, USA). The procedure consisted of rapid mixing at 200 rpm for 2 min (coagulant addition and flash mixing), followed by slow mixing at 30 rpm for 20 min (flocculation), and a quiescent settling period of 30 min. After settling, supernatant samples were collected from a depth of 5 cm below the surface for analysis of turbidity, colour, COD, and TSS.

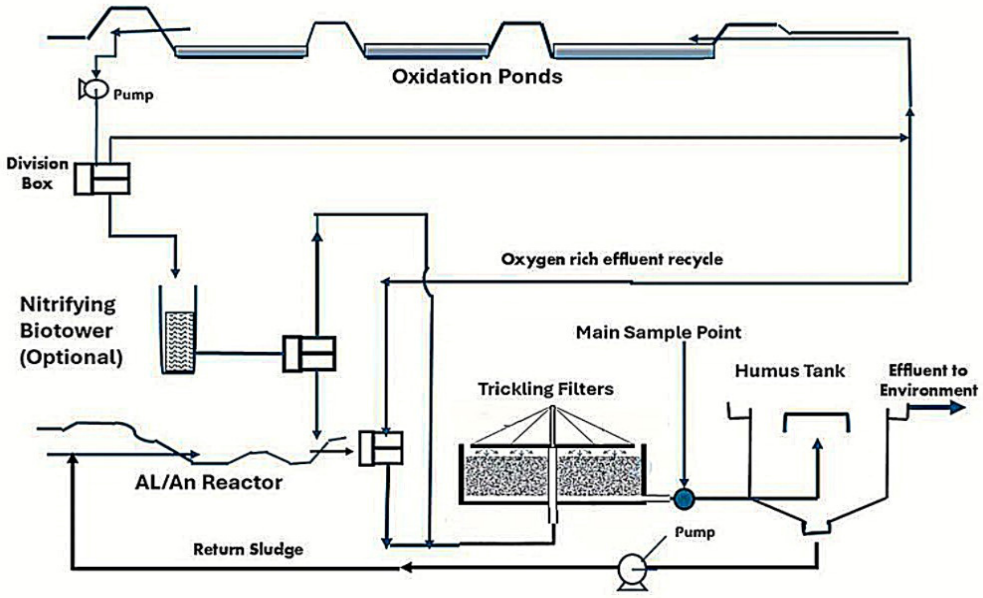

Figure 2. The Schematic diagram of the Pond Enhanced Treatment and Operation (PETRO) System at Palapye wastewater treatment plant.

All collected samples were stored in a cold room maintained at a temperature range of 6 to 8 °C and analysed immediately upon arrival at the laboratory.

The Pond Enhanced Treatment and Operation (PETRO) system is an integrated wastewater treatment process that combines natural and engineered systems to effectively treat sewage and industrial effluents. The system typically includes oxidation ponds, where algae and aerobic bacteria work synergistically to degrade organic matter. A nitrifying biotower facilitates the conversion of ammonia to nitrates, while a trickling filter further breaks down pollutants through a biofilm of microorganisms. Settled biological solids are removed in a humus tank, and an Anaerobic/Anoxic (AL/An) pond reactor promotes denitrification and anaerobic digestion, converting nitrates to nitrogen gas and breaking down organic matter in oxygen-deprived conditions. This multi-stage approach ensures comprehensive removal of organic pollutants, nutrients, and pathogens, making the PETRO system a robust solution for sustainable wastewater treatment.

The pH range for the CCD (8.38–12.6) was selected based on preliminary experiments that identified optimal turbidity removal above pH 11, coupled with the known precipitation pH for magnesium hydroxide (pH > 10.5) and calcium carbonate (pH > 9.5). Given the secondary effluent's hardness concentration (180–220 mg/L as $CaCO_3$), this range was chosen to systematically evaluate the synergistic effects of pH-induced precipitation softening and coagulant addition.

2.2. Materials

The following materials were used in this study: Aluminium sulphate octadecahydrate ($Al_2(SO_4)_3.18H_2O$) from Sigma-Aldrich Inc., St. Louis, MO, USA (Lot number BCBX4913), Iron (III) chloride hexahydrate ($FeCl_3.6H_2O$) from Sigma-Aldrich (Lot number STBJ3986) and Organic *Moringa oleifera* powder (Batch 20003, imported and marketed by Moringa Technology Industry, Gaborone, Botswana). Nitric acid (HNO_3) from Sigma-Aldrich Inc., St. Louis, MO, USA (Lot number MKCJ9713). Sodium hydroxide (NaOH) from Sigma-Aldrich (Lot number SLCC8729). All chemicals were of analytical grade.

Moringa oleifera seeds were obtained from community-based suppliers and small-scale growers in Botswana. The seeds were dehusked manually, and the kernels were dried at 60 °C for 24 h in a laboratory oven. The dried kernels were ground using a laboratory grinder and sieved to a particle size of <0.5 mm. The resulting powder was stored in airtight containers at room temperature until use. No chemical extraction or purification was performed; the crude powder was used directly as the natural coagulant.

2.3. Statistical Analysis and Model Evaluation

Statistical analysis was performed using Design Expert software (Version 12, Stat-Ease, Minneapolis, MN, USA). Polynomial models were fitted to the experimental data, and model selection was guided by FIT statistics, including R^2, adjusted R^2, predicted R^2, and adequate precision. Model terms with p-values < 0.05 were considered statistically significant. Analysis of Variance (ANOVA) was used to assess overall model significance, with F-tests evaluating regression coefficients. The lack-of-FIT test was examined to ensure model adequacy, and diagnostic plots (normal probability plots, residuals vs. predicted, etc.) were used to verify ANOVA assumptions.

In addition to the diagnostic statistics generated by Design Expert software (Version 12), external validation was performed using 3 independent experimental runs (not included in the original 39-run CCD). These validation experiments were conducted at random points within the design space, and predicted values from the regression models were compared with actual measured values using percent error and root mean square error (RMSE) calculations. Additionally, residual analysis was performed to check for homoscedasticity and normal distribution of errors.

Model Graphs

Model graphs were employed to aid in interpreting the selected model. A 3D Surface plot illustrated how the response varied as factors changed in a three-dimensional display encompassing the actual design points. These plots depicted the impact of $Al_2(SO_4)_3.18H_2O$, $FeCl_3.6H_2O$, and Moringa dosage on turbidity, colour, COD, and TSS as pH and dosage changed.

2.4. Quality Assurance and Replication

All jar test experiments were conducted in triplicate to ensure reproducibility, and results are reported as mean ± standard deviation. Laboratory blanks and control samples (without coagulant) were included in each experimental run. Analytical measurements followed [12] with appropriate quality controls: turbidity was measured using a calibrated

Hach 2100N turbidimeter (Hach Company, Loveland, CO, USA) with daily verification against standard formazin suspensions; COD analyses included potassium hydrogen phthalate standards and blank corrections; TSS determinations used pre-weighed glass fibre filters (Whatman GF/C Maidstone, Kent, UK) dried at 105 °C to constant weight. Instrument calibration was verified before each analytical batch.

2.5. Final Equation in Terms of Coded and Actual Factors

The regression computations were performed using the coded scale, allowing predictions about the response for specific factor levels. High levels were coded as +1, and low levels as −1 by default. The coded equation was valuable for comparing factor coefficients' relative impact. Subsequently, the coded model was converted to the actual model, represented by the final equation in terms of actual factors.

2.6. Apllication of Response Surface Methodology

The data acquired from preliminary studies were employed in conjunction with the Central Composite Design (CCD, rotatable) and Response Surface Methodology (RSM) to optimise coagulation and flocculation parameters. The efficiency of pollutant removal was calculated using the following equation:

$$\eta = \frac{\left(C_i - C_f\right)}{C_i} \times 100\% \quad (1)$$

where

C_i = the initial concentration

C_f = the final concentration

The limitations of the one-factor-at-a-time OFAT) approach, including its time and resource-intensive nature, limited statistical analysis, and inability to bridge gaps between tested values, prompted the adoption of Response Surface Methodology (RSM). RSM is a statistical technique capable of comprehensively evaluating experimental data and developing mathematical models [13,14].

It is worth noting that Machlor et al. [14] highlighted the scarcity of studies utilising RSM to model coagulant dosage. In the literature, RSM has been applied with various experimental designs, including the Box–Behnken design [15], Central Composite Design (CCD) [13,16], and Uniform Design (UD) [17]. The primary objective of our Design of Experiment (DOE) was to determine factor settings that maximise the removal efficiency of turbidity, colour, Chemical Oxygen Demand (COD), and Total Suspended Solids (TSS) for optimising the treatment process.

To achieve this, we employed Central Composite Design (CCD) and Response Surface Methodology (RSM) using Design Expert (DX) software version 12, obtained from StatEase, Minneapolis, MN, USA. The categorical factor in our study consisted of three levels: $Al_2(SO_4)_3 \cdot 18H_2O$, $FeCl_3 \cdot 6H_2O$, and *Moringa oleifera*. These coagulants were evaluated based on their effectiveness in achieving optimum dosage and pH for turbidity, colour, COD, and TSS removal. The equation model used for predicting the optimal conditions is as follows [18]:

$$Y = \beta_0 + \sum_{i=1}^{k} \beta_i X_i + \sum_{i=1}^{k} \beta_{ii} X_i^2 + \sum_{i=1}^{k-1} \sum_{j=i+1}^{k} \beta_{ij} X_i X_j + \varepsilon \quad (2)$$

where

Y—Predicted response (dependent variable).

β_i—represents the linear coefficient.

j—represents the quadratic coefficient.

β_0—represents the Intercept coefficient.

X_i, X_j—Independent variables (factors).

β_{ii}—represents the quadratic effect (curvature) of the independent variable X_i on the response.

X_i^2—the squared value of the independent variable X_i, accounting for non-linear relationships.

β_{ij}—represents the interaction effect between independent variables X_i and X_j on the response.

X_iX_j—the product of independent variables X_i and X_j, accounting for synergistic or antagonistic effects.

k—Number of independent variables (factors) studied and optimised in the experiment represents the random error.

i, j—denote specific independent variables.

We conducted a total of 39 experimental runs, as recommended by CCD for robust design purposes. Table 1 presents the actual and coded values for the independent variables and their respective levels used in the RSM and CCD experimental design:

Table 1. Actual and coded values for the independent variables and their levels for RSM and CCD experimental design.

Input Variable	Numeric Factor Levels				
	−1.414	**−1**	**0**	**+1**	**+1.414**
	Lower	**Low**	**Centre**	**High**	**Higher**
pH	8.38	9	10.5	12	12.6
$Al_2(SO_4)_3.18H_2O$, mg/L	2.93	5	10	15	17.1
$FeCl_3.6H_2O$, mg/L	5.86	10	20	30	34.1
Moringa oleifera, mg/L	0.76	2	5	8	9.2

2.7. Economic Analysis Methodology

Cost analysis was performed based on local market prices in Botswana as of September 2020. Coagulant costs were obtained from major chemical suppliers in Gaborone: $FeCl_3 \cdot 6H_2O$ at USD 1800/ton (bulk industrial grade), $Al_2(SO_4)_3 \cdot 18H_2O$ at USD 1550/ton, and *Moringa oleifera* seed powder at USD 650/ton (processed locally). Operational costs were calculated using Equation (3) [19].

$$OC = (P_c \times D_c) + C_e + C_s \quad (3)$$

where OC = Total operating cost per unit volume treated (USD/m^3), P_c = Coagulant unit price (USD/ton), D_c = Coagulant dosage (ton/m^3), C_e = Energy cost for rapid and slow mixing (USD/m^3) and C_s = Sludge handling and disposal cost (USD/m^3).

Energy costs were estimated based on 0.05 kWh/m^3 for rapid mixing (1 min at 100 rpm) and 0.02 kWh/m^3 for flocculation (20 min at 30 rpm), with electricity at USD 0.10/kWh. Sludge production was estimated at 0.5 kg dry solids/m^3 treated, with disposal costs of USD 50/ton (dewatered sludge). Capital costs for dosing equipment (pumps, tanks, controls) were estimated at USD 15,000–20,000 based on quotations from local equipment suppliers. All costs are presented in 2020 USD.

3. Results

3.1. Preliminary Experiments

Preliminary studies were conducted to establish the optimum conditions for coagulation and flocculation using aluminium sulphate ($Al_2(SO_4)_3 \cdot 18H_2O$), ferric chloride ($FeCl_3 \cdot 6H_2O$), and *Moringa oleifera* seed extract. The initial stage focused on identifying the optimum pH for turbidity removal [14,20].

As shown in Table 2, turbidity removal efficiency increased with increasing pH for all three coagulants, confirming that coagulation–flocculation performance is strongly influenced by pH. Ferric chloride exhibited the highest removal efficiencies across most pH levels, reaching nearly 99% at pH 12.4. *Moringa oleifera* showed comparable removal to ferric chloride at alkaline pH (>9), while aluminium sulphate demonstrated effective removal across a broader pH range, achieving over 90% at pH 12.2. This trend aligns with observations by [19–21], who reported enhanced coagulation–flocculation with increasing pH.

Table 2. Comparative data on the efficiency of $Al_2(SO_4)_3.18H_2O$, $FeCl_3.6H_2O$, and *Moringa oleifera* coagulants in filtered turbidity removal across pH levels.

$Al_2(SO_4)_3.18H_2O$		$FeCl_3.6H_2O$		Moringa	
pH	**% Turbidity Removal**	**pH**	**% Turbidity Removal**	**pH**	**% Turbidity Removal**
2.0	46.5	2.0	70.0	2.0	69.2
3.5	62.3	3.0	75.6	4.0	63.8
6.1	76.0	6.1	85.6	6.1	76.1
7.1	84.3	9.6	92.0	9.0	96.4
11.0	81.5	11.8	96.9	11.1	97.7
12.2	92.7	12.4	98.9	12.4	98.5

The improvement in turbidity removal with pH adjustment can be explained by charge neutralisation. As NaOH is added, sodium ions (Na^+) increase in solution, reducing electrostatic repulsion among colloidal particles and promoting aggregation and settling [22,23]. This explains why turbidity removal at 0 mg/L coagulant dosage was not 0% (Figures 3–5); the sodium ions themselves induced partial coagulation even without added coagulant.

Correlation analysis between pH and turbidity removal (Figure 3) further illustrates these differences. Ferric chloride showed the strongest linear correlation (R^2 = 0.9805), indicating a highly pH-sensitive mechanism. *Moringa oleifera* also demonstrated a strong relationship (R^2 = 0.879), while aluminium sulphate exhibited a moderate dependence (R^2 = 0.819). These findings highlight the importance of both coagulant choice and pH optimisation in maximising turbidity removal, with ferric chloride being the most pH-responsive.

It is important to note that the removal efficiencies presented in Tables 3–5 and Figures 4–6 represent the combined effect of two mechanisms: (1) baseline removal from pH-induced precipitation of hardness ions (Mg^{2+}, Ca^{2+}) as $Mg(OH)_2$ and $CaCO_3$, which occurs even at 0 mg/L coagulant dose; and (2) incremental removal attributable to the added coagulants. For example, in Table 4, the baseline turbidity removal at 0 mg/L $FeCl_3 \cdot 6H_2O$ is 99.3%, increasing marginally to 99.5% at 100 mg/L. This demonstrates that the primary driver of treatment at high pH is precipitation softening, with coagulants providing modest but meaningful refinement of floc structure and settling characteristics. The incremental benefit of coagulant addition becomes more evident in parameters like TSS removal, which increased from 93.3% (0 mg/L) to 100% (50 mg/L $FeCl_3 \cdot 6H_2O$).

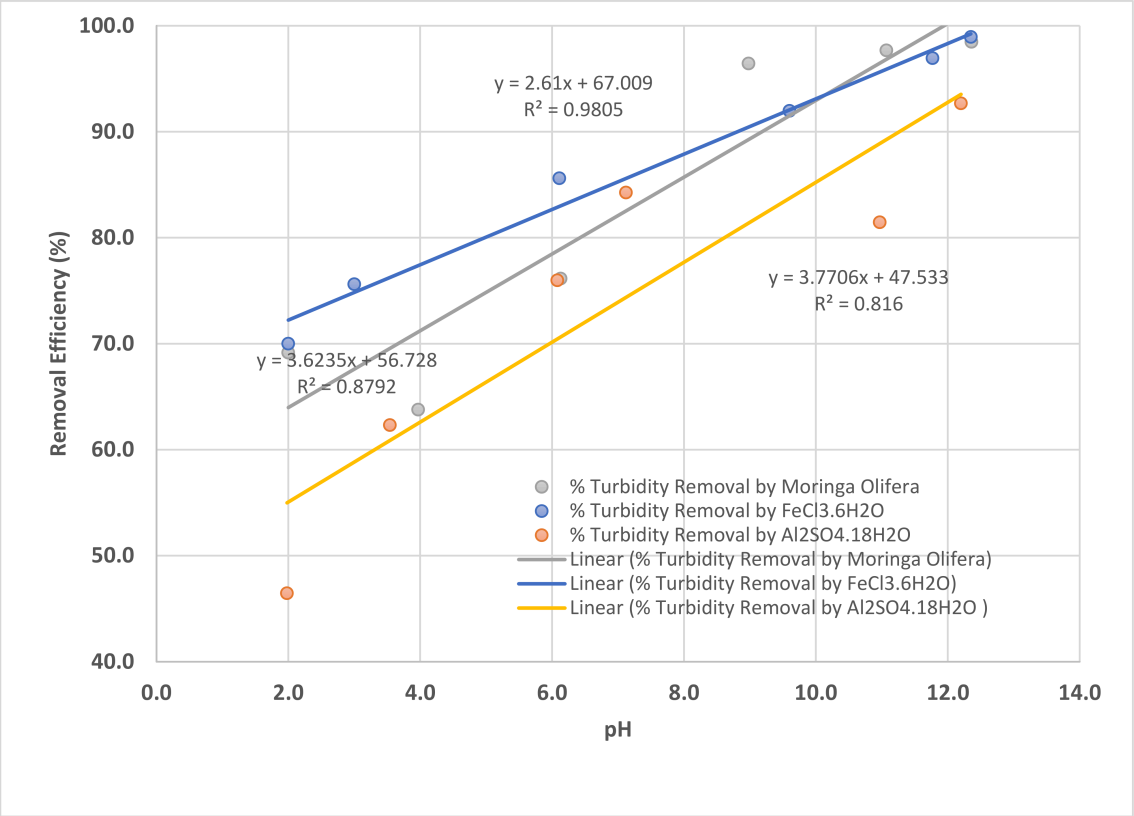

Figure 3. Combined effect of pH-induced precipitation and coagulant addition on turbidity removal efficiency for $Al_2(SO_4)_3 \cdot 18H_2O$, $FeCl_3 \cdot 6H_2O$, and *Moringa oleifera* across varying pH levels. The removal at each pH represents the synergistic action of NaOH-driven precipitation of hardness ions and coagulant-mediated flocculation.

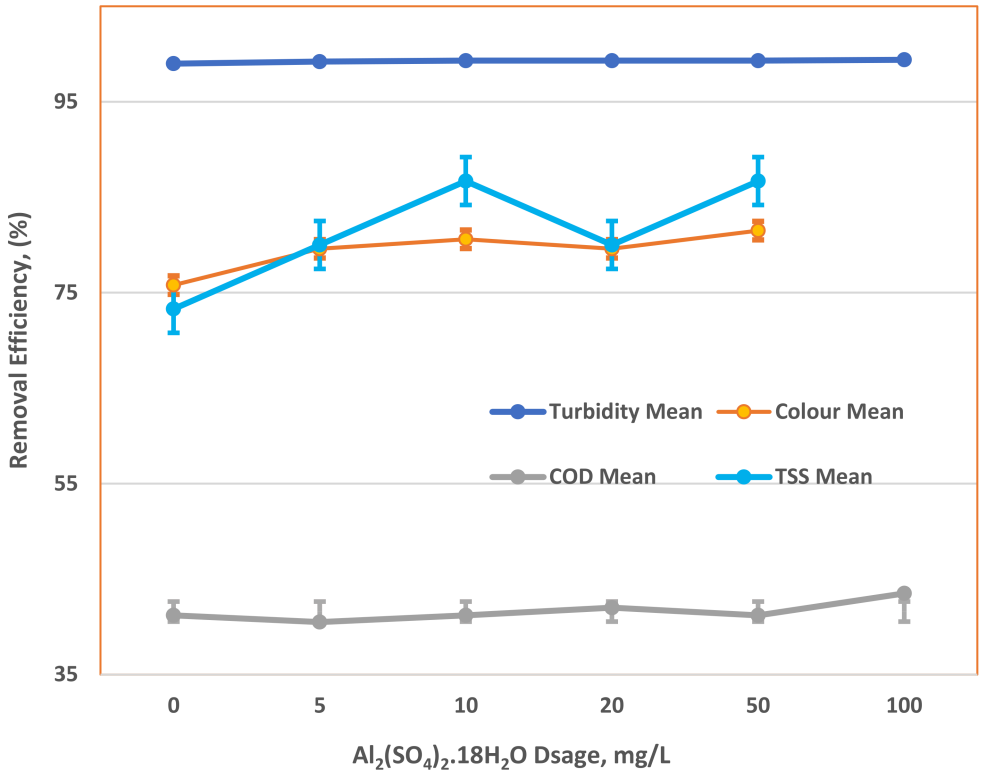

Figure 4. Pollutant removal efficiency for varying dosages of $Al_2(SO_4)_3 \cdot 18H_2O$ (0–100 mg/L) at optimum pH, showing removal percentages for turbidity, colour, COD, and TSS.

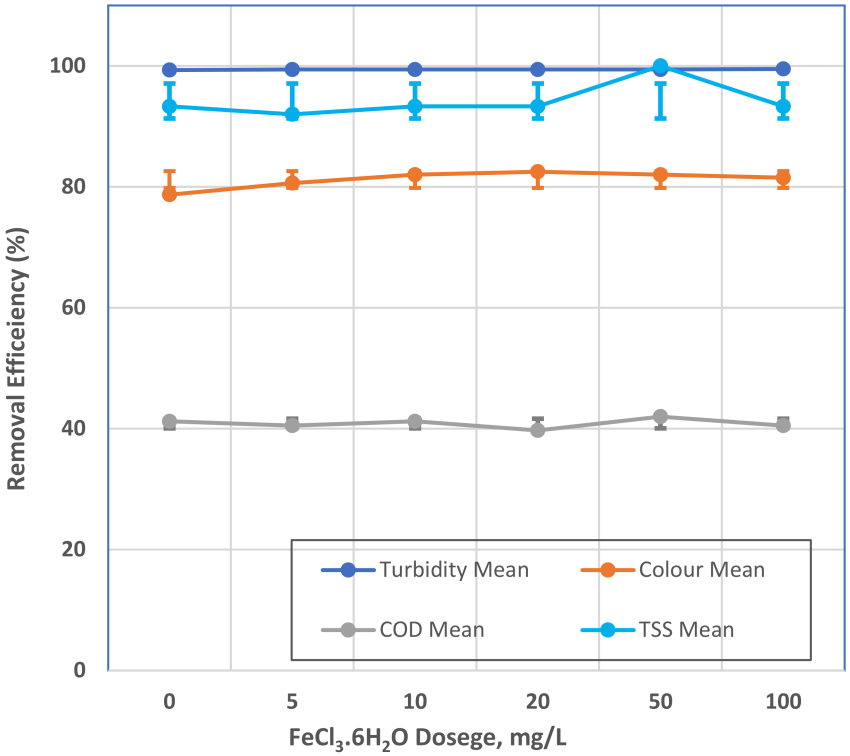

Figure 5. Pollutant removal efficiency for varying dosages of $FeCl_3 \cdot 6H_2O$ (0–100 mg/L) at optimum pH, showing removal percentages for turbidity, colour, COD, and TSS.

Table 3. Pollutant removal efficiency for varying dosages of $Al_2(SO_4)_3 \cdot 18H_2O$ (0–100 mg/L) at optimum pH.

Dosage (mg/L)	Final Turbidity (NTU)	Final Colour (mg/L Pt–Co)	Final COD (mg/L O_2)	Final TSS (mg/L)	COD Removal (%)	TSS Removal (%)	Turbidity Removal (%)	Colour Removal (%)
0	0.12	51	77	4	41.2	73.3	99.0	75.8
5	0.095	43	78	3	40.5	80.0	99.2	79.6
10	0.09	41	77	2	41.2	86.7	99.3	80.6
20	0.09	43	76	3	42.0	80.0	99.3	79.6
50	0.09	39	77	2	41.2	86.7	99.3	81.5
100	0.08	42	74	1	43.5	93.3	99.4	80.1

Raw Data: Turbidity 12.4 NTU, Colour 211 mg/L Pt–Co, COD 131 mg/L O_2, TSS 15 mg/L.

Table 4. Pollutant removal efficiency for varying dosages of $FeCl_3 \cdot 6H_2O$ (0–100 mg/L) at optimum pH.

Dosage (mg/L)	Final Turbidity (NTU)	Final Colour (mg/L Pt–Co)	Final COD (mg/L O_2)	Final TSS (mg/L)	COD Removal (%)	TSS Removal (%)	Turbidity Removal (%)	Colour Removal (%)
0	0.085	45	77	1	41.2	93.3	99.3	78.7
5	0.07	41	78	3	40.5	80.0	99.4	80.6
10	0.07	38	77	1	41.2	93.3	99.4	82.0
20	0.07	37	79	1	39.7	93.3	99.4	82.5
50	0.07	38	76	0	42.0	100.0	99.4	82.0
100	0.06	39	78	1	40.5	93.3	99.5	81.5

Raw Data: Turbidity 12.4, Colour 211, COD 131, TSS 15.

Table 5. Pollutant removal efficiency for varying dosages of *Moringa oleifera* powder (0–100 mg/L) at optimum pH.

Dosage (mg/L)	Final Turbidity (NTU)	Final Colour (mg/L Pt–Co)	Final COD (mg/L)	Final TSS (mg/L)	Turbidity Removal (%)	Colour Removal (%)	COD Removal (%)	TSS Removal (%)
0	0.09	49	82	3	99.3	76.8	37.4	80.0
5	0.07	48	81	2	99.4	77.3	38.2	86.7
10	0.08	51	83	2	99.4	75.8	36.6	86.7
20	0.09	61	85	4	99.3	71.1	35.1	73.3
50	0.11	73	96	2	99.1	65.4	26.7	86.7
100	0.165	117	106	6	98.7	44.5	19.1	60.0

Raw Data: Turbidity 12.4, Colour 211, COD 131, TSS 15.

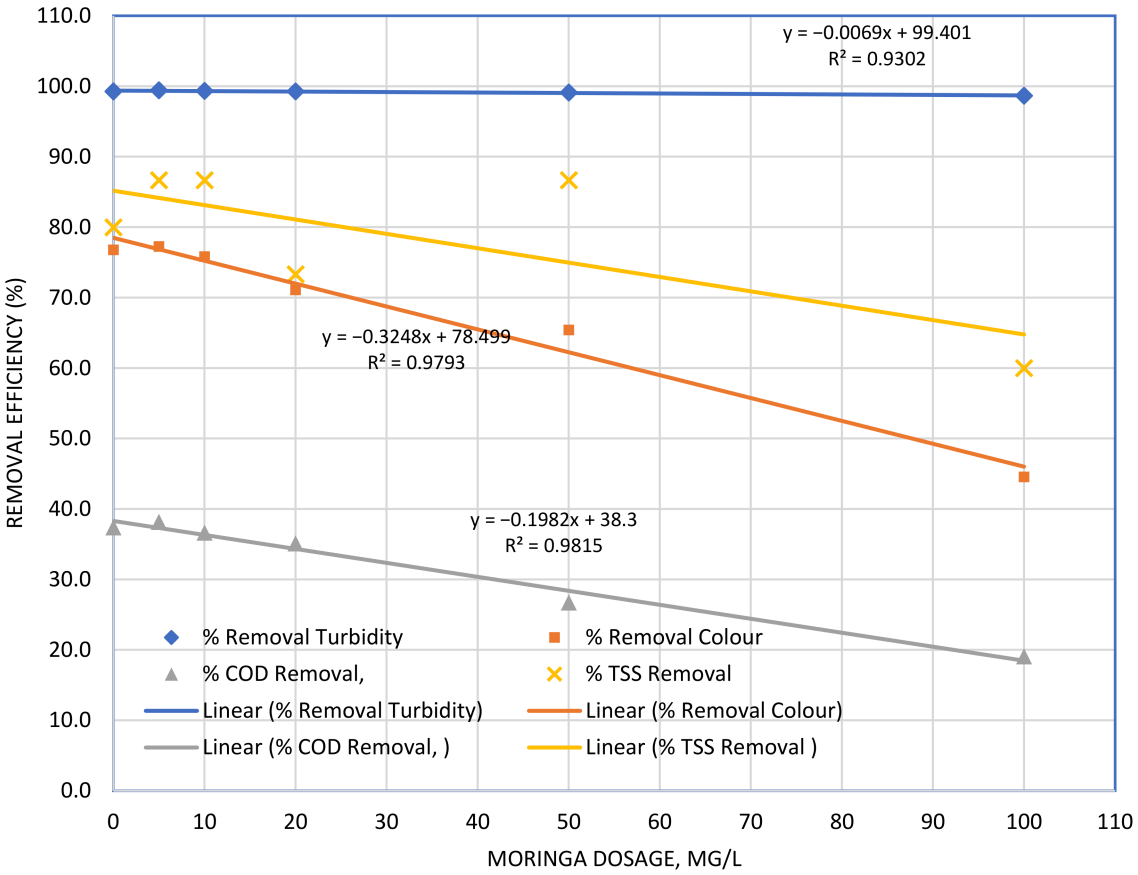

Figure 6. Pollutant removal efficiency for varying dosages of *Moringa oleifera* powder (0–100 mg/L) at optimum pH, showing removal percentages for turbidity, colour, COD, and TSS.

In addition to turbidity, removal of Colour, COD, and TSS was evaluated across varying coagulant dosages at optimum pH. Table 3 and Figure 4 present the performance of aluminium sulphate. Turbidity removal exceeded 99% at dosages above 10 mg/L, while Colour and COD removals were consistently above 80% and 40%, respectively. TSS removal reached over 90% at higher dosages. This demonstrates that aluminium sulphate is highly effective in reducing particulate matter and Colour, with modest performance in COD reduction.

Similarly, Table 4 and Figure 5 show the performance of ferric chloride. High turbidity removal (≥99%) was observed even at the lowest tested dosage, while Colour removal steadily increased to 82% at 20–50 mg/L. COD removal remained in the range of 40–42%,

with TSS removal reaching up to 100% at 50 mg/L. These results confirm ferric chloride's superior capacity for turbidity and TSS reduction, although COD removal remained moderate.

The performance of *Moringa oleifera* as a natural coagulant is summarised in Table 5 and Figure 6. At low dosages (≤10 mg/L), *Moringa oleifera* achieved turbidity removal above 99% and Colour removal around 75–77%. However, at higher dosages (>20 mg/L), its efficiency declined, with turbidity removal dropping to 98.7% and Colour removal decreasing to as low as 44.5% at 100 mg/L. COD and TSS removals also decreased with higher dosage, suggesting that overdosing with *Moringa oleifera* leads to particle restabilisation or re-dispersion due to excess organic matter from the coagulant itself.

Overall, the preliminary experiments (Table 5 and Figure 6) demonstrate that ferric chloride is the most consistent coagulant across parameters, providing high turbidity and TSS removal over a wide dosage and pH range. Aluminium sulphate performs comparably for turbidity and Colour removal, but with slightly lower COD removal efficiency. *Moringa oleifera*, although highly effective at low dosages, shows reduced efficiency at higher concentrations, indicating the need for careful dosage optimisation when using it as a sustainable, natural alternative.

3.2. Response Surface Methodology

Table 6 presents the characterisation of trickling filter (TF) effluent and the pH levels for the stock solution. The preparation of stock solutions for the coagulants involved weighing 10 g of each coagulant and dissolving it in a 1000 mL volumetric flask filled with tap water. However, it is important to note that due to *Moringa oleifera*'s tendency to float in water, the 1000 mL of water was transferred into a beaker for the solution to be prepared effectively.

Table 6. Trickling filter effluent characterisation and pH of coagulant stock solutions.

Parameter	Unfiltered	Filtered (0.45 µm)
Trickling filter effluent		
Turbidity (NTU)	50.7	4
Colour (mg/L Pt-Co)	762	147
COD (mg/L O_2)	202	-
TSS (mg/L)	65	-
Coagulant Stock Solution (10 g/L)	pH	
$Al_2(SO_4)_3 \cdot 18H_2O$	3.7	
$FeCl_3 \cdot 6H_2O$	2.12	
Moringa oleifera	6.25	

3.2.1. Descriptive and FIT Statistics

In Table 7, we present the descriptive and FIT statistics for our models. The evaluation of these models is based on *p*-values, where *p*-values less than 0.05 indicate that model terms are significant, while values greater than 0.10 suggest that the model terms are not significant. For our turbidity model, we identified that the terms A, B, C, AB, AC, and A^2 are significant model terms. Additionally, the BC term was included to maintain the hierarchy of the model. The Model F-value of 111.47 indicates the significance of the model, with only a 0.01% chance that such a large F-value could occur due to random noise.

Table 7. Summary of descriptive and model fit statistics for response surface models.

Response	Model		Lack-of-Fit		FIT Statistics			
	F Values	*p* Value	F Value	*p* Value	R^2	Adj R^2	Pred. R^2	Adq. Precision
Turbidity	114.47	<0.0001	1.7	0.1789	0.9764	0.9676	0.9481	41.4541
Colour	244.43	<0.0001	1.58	0.2161	0.9869	0.9828	0.9796	66.5861
COD	118.25	<0.0001	1.71	0.1834	0.9718	0.9636	0.9456	47.2574
TSS	21.22	<0.0001	0.9832	0.5234	0.8908	0.8488	0.7668	16.2008

To assess the acceptability of our models, we employed several criteria, including: (1) the difference between the Predicted R^2 and Adjusted R^2, and (2) the signal-to-noise ratio measured by Adequate Precision. For the turbidity model, we determined its acceptance by evaluating the difference between the Predicted R^2 (0.9481) and the Adjusted R^2 (0.9676). The resulting difference of 0.0195 was found to be less than the threshold of 0.2, indicating the model's suitability. Additionally, we measured the signal-to-noise ratio for this model, which resulted in a ratio of 41.454, significantly exceeding the threshold of 4. This high ratio signifies that the model provides an adequate signal for navigating the design space.

In assessing the lack-of-fit test, our goal is for the model to fit the data well. The lack-of-fit F-value of 1.70 suggests that the lack-of-fit is not significant in comparison to the pure error. There is a 17.89% chance that a lack-of-fit F-value of this magnitude could occur due to random noise. These statistical analyses provide valuable insights into the significance and goodness-of-fit of our models, helping us make informed decisions regarding their utility and reliability.

Similar assessments were conducted for the remaining models, ensuring that all met the necessary criteria for acceptance. These rigorous evaluations confirm the reliability of our models and their effectiveness in guiding our research and design processes. The complete experimental design matrix comprising the 39 runs with the actual factor levels and corresponding response values is provided in Table S1 of the Supplementary Materials. Furthermore, the detailed ANOVA tables, including the significance of each individual model term ($p < 0.05$) for all four responses, are presented in Tables S2–S5. The complete experimental design matrix comprising the 39 runs with the actual factor levels and corresponding response values is provided in Table S1 of the Supplementary Materials.

3.2.2. Response Surface Visualisation

To visualise the interaction effects between pH and coagulant dosage on pollutant removal, three-dimensional response surface plots were generated from the quadratic models. Figure 7 presents the response surfaces for turbidity, colour, COD, and TSS removal using $FeCl_3 \cdot 6H_2O$ at its optimal dosage range. The curvature of the surfaces confirms the significant quadratic effects identified in the ANOVA (see Tables S2–S5 in Supplementary Materials), while the elliptical shape of the contours indicates the presence of interaction between pH and dosage. The steep ascent in the turbidity surface (Figure 7a) towards higher pH values (>11) and mid-range dosages (20–30 mg/L) visually corroborates the strong pH sensitivity observed in preliminary studies (Section 3.1). Similar patterns are evident for colour and TSS, while the COD surface exhibits a broader plateau, reflecting its more modest response to coagulation.

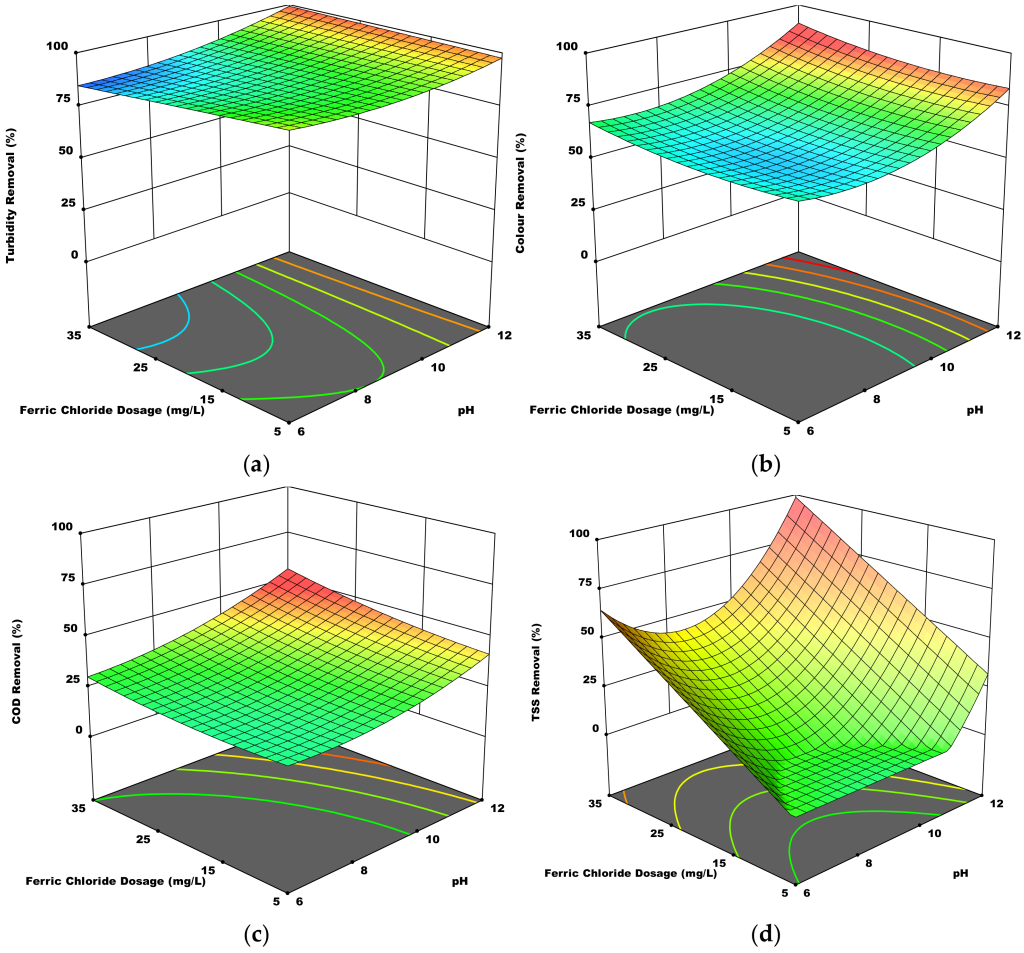

Figure 7. 3D response surface plots of removals by $FeCl_3 \cdot 6H_2O$ for (**a**) turbidity, (**b**) colour, (**c**) COD, and (**d**) TSS. The color gradient (blue to red) represents the percentage removal, where blue indicates lower removal efficiency and red indicates higher removal efficiency. Contour lines on the surface represent lines of equal removal percentage. The x- and y-axes represent pH and coagulant dosage (mg/L), respectively.

3.2.3. Multi-Response Optimisation and Confirmation

Multi-response optimisation using desirability functions was performed to identify compromise conditions balancing all four water quality parameters. The individual desirability values ranged from 0.92 to 0.97, indicating excellent agreement between predicted and target responses. Confirmation runs (n = 3) were conducted at the optimal conditions identified for each coagulant: for $FeCl_3 \cdot 6H_2O$ (pH 12.0, 30 mg/L), the experimental results showed deviations of less than 5% from model predictions (turbidity: 94.2% predicted vs. 93.8% actual; colour: 89.5% vs. 88.9%; COD: 63.2% vs. 62.5%; TSS: 92.1% vs. 91.4%), confirming the robustness and predictive capability of the developed models.

3.3. External Model Validation

The regression models were validated using 3 independent experimental runs. The predicted versus actual values for key responses are summarised in Table 8. The average percent error for turbidity, colour, COD, and TSS predictions were 3.2%, 4.8%, 7.1%, and 5.5%, respectively, with corresponding RMSE values of 0.41 NTU, 8.7 mg/L Pt-Co, 5.2 mg/L O_2, and 1.8 mg/L. These low error metrics confirm the models' robustness and predictive capability within the defined design space.

Table 8. Comparison of predicted values from the quadratic regression models with actual measured values from three independent validation experiments.

Run	Parameter	Predicted Value	Actual Value	Percent Error (%)	RMSE *
1	Turbidity (NTU)	0.45	0.47	4.3	0.41 NTU
	Colour (mg/L Pt-Co)	42.1	44.5	5.4	8.7 mg/L
	COD (mg/L O_2)	58.3	62.8	7.2	5.2 mg/L
	TSS (mg/L)	3.2	3.4	5.9	1.8 mg/L
2	Turbidity (NTU)	0.38	0.36	5.6	0.41 NTU
	Colour (mg/L Pt-Co)	38.7	40.2	3.7	8.7 mg/L
	COD (mg/L O_2)	61.5	65.1	5.5	5.2 mg/L
	TSS (mg/L)	2.8	2.9	3.4	1.8 mg/L
3	Turbidity (NTU)	0.52	0.50	4.0	0.41 NTU
	Colour (mg/L Pt-Co)	45.3	47.8	5.2	8.7 mg/L
	COD (mg/L O_2)	55.8	60.3	7.5	5.2 mg/L
	TSS (mg/L)	3.5	3.7	5.4	1.8 mg/L
Average	All Parameters	-	-	5.4	-
Overall RMSE	-	-	-	-	See below

* Overall, Root Mean Square Error (RMSE): Turbidity = 0.41 NTU; Colour = 8.7 mg/L **Pt–Co**; COD = 5.2 mg/L O_2; TSS = 1.8 mg/L.

3.4. Residual Metal Concentrations

This study focused on the primary treatment objectives of turbidity, colour, COD, and TSS removal. Residual concentrations of aluminium and iron in the treated effluent were not measured. This represents a limitation, as elevated residual metals could pose ecotoxicological risks to the receiving Lotsane dam ecosystem and may be subject to regulatory limits under Botswana's effluent discharge standards [4]. The need for this analysis is addressed in Section 4.5.

3.5. Economic Analysis Results

The economic analysis was performed using the methodology described in Section 2.7, with all costs presented in 2020 USD. Table 9 summarises the operational costs for each coagulant at their respective optimal conditions identified through multi-response optimisation.

Table 9. Comparative economic analysis of coagulants at optimal conditions.

Parameter	$Al_2(SO_4)_3 \cdot 18H_2O$	$FeCl_3 \cdot 6H_2O$	*Moringa oleifera*
	Optimal Conditions		
pH	12.0	12.0	12.0
Dosage (mg/L)	15	30	8
	Cost Components (USD/m^3)		
Coagulant cost	0.0233	0.0540	0.0052
Energy cost (mixing)	0.007	0.007	0.007
Sludge handling/disposal	0.025	0.028	0.022
Total Operational Cost (USD/m^3)	0.0553	0.0890	0.0342
Annual Cost (USD/year) for 2000 m^3/day	40,369	64,970	24,966
Capital Cost (dosing equipment)	15,000–18,000	15,000–20,000	15,000–18,000

Notes: Annual cost calculated based on 2000 m^3/day design flow (Palapye plant capacity) and 365 days of operation. Energy costs assume 0.07 kWh/m^3 total at USD 0.10/kWh. Sludge production estimated at 0.45–0.55 kg dry solids/m^3 with disposal at USD 50/ton.

The analysis reveals that while *Moringa oleifera* offers the lowest operational cost (USD 0.0342/m^3), this must be balanced against its narrower optimal dosage window and lower COD removal efficiency (56.6% vs. 63.8% for $FeCl_3 \cdot 6H_2O$). Ferric chloride, despite having the highest operational cost (USD 0.0890/m^3), provides the most consistent and robust performance across all parameters, with TSS removal reaching 100% at optimal dosage. Aluminium sulphate offers an intermediate option with moderate cost (USD 0.0553/m^3) and reliable performance.

The capital investment for dosing equipment (USD 15,000–20,000) is modest compared to the cost of major plant upgrades or potential non-compliance penalties. For the Palapye facility, which has consistently failed to meet discharge standards, the incremental operational cost of USD 0.034–0.089 per m^3 represents a cost-effective solution for achieving regulatory compliance.

4. Discussion

4.1. Interpretation of Coagulant Performance and Mechanisms

The comparative evaluation of $Al_2(SO_4)_3 \cdot 18H_2O$, $FeCl_3 \cdot 6H_2O$, and *Moringa oleifera* seed powder within a single RSM-CCD framework revealed distinct performance profiles and mechanistic behaviours. The superior turbidity and TSS removal efficiency of $FeCl_3$, particularly at high pH, aligns with established literature on ferric salts, which are effective across a broad pH range due to the formation of highly charged polymeric species like $Fe(OH)_3^+$ that enhance charge neutralisation and sweep flocculation [7,24]. The strong linear correlation (R^2 = 0.9805) between pH and turbidity removal for $FeCl_3$ underscores its high pH-sensitivity, likely due to the increased precipitation of ferric hydroxide at alkaline conditions, which enmeshes colloidal particles.

Conversely, the performance decline of *Moringa oleifera* at dosages exceeding 20 mg/L is a critical finding. This phenomenon, where increasing coagulant dosage reduces removal efficiency, is characteristic of restabilisation via charge reversal [5,25]. *Moringa oleifera* proteins (cationic polypeptides) initially neutralise negatively charged particles. However, excess dosage can lead to an overall positive charge on particle surfaces, reinstating electrostatic repulsion and causing dispersion [8,25]. Furthermore, the leaching of soluble organic matter from the *Moringa oleifera* powder at high doses may increase the soluble COD and colour of the effluent, as observed in our results (Table 5). This highlights a significant operational constraint for natural coagulants: their optimal dosage window is narrow and must be precisely controlled, unlike the broader effective ranges of metal-based coagulants. Alum demonstrated consistent, robust performance, particularly for turbidity and colour removal. Its mechanism is primarily based on the formation of $Al(OH)_3$ precipitates that adsorb and entrain contaminants. Its moderate pH dependence (R^2 = 0.819) suggests effective performance across a wider operational pH band, making it a reliable, if less pH-optimised, alternative to $FeCl_3$ for the parameters studied.

The residual COD (40–60 mg/L) represents soluble, non-settleable organic matter that remains after coagulation, consistent with coagulation's inherent limitations. Coagulation-flocculation is primarily effective at removing particulate and colloidal organic matter, while soluble COD fractions (such as low molecular weight organic acids and carbohydrates) are not efficiently removed by this mechanism. This explains why COD removal efficiencies (56.6–63.8%) were consistently lower than turbidity and TSS removals (>90%) across all coagulants tested.

Coagulation vs. pH-Induced Precipitation at Alkaline pH

The optimal pH range identified in this study (pH 12–12.6) exceeds the classical optima for hydrolysing metal salts, where Al^{3+} and Fe^{3+} typically form insoluble hydroxide flocs

(pH 5.5–7.5 for Al; pH 4–11 for Fe) [15,17]. At pH > 11, aluminium exists predominantly as soluble aluminate ions ($Al(OH)_4^-$), incapable of forming $Al(OH)_3$(s) precipitates for sweep flocculation. The significant pollutant removal observed at 0 mg/L coagulant dose across all coagulants (e.g., 99.0–99.3% turbidity removal in Tables 3–5) demonstrates that pH elevation alone, via NaOH addition, is a primary driver of treatment. This baseline removal is attributed to pH-induced precipitation of native hardness ions (Ca^{2+}, Mg^{2+}) present in the secondary effluent. At pH > 11, magnesium hydroxide ($Mg(OH)_2$(s)) and calcium carbonate ($CaCO_3$(s)) precipitate rapidly, forming voluminous microcrystalline flocs that enmesh suspended particles and organic matter through a sweeping mechanism [25,26]. Thus, the process at zero coagulant dose is better characterised as enhanced precipitation softening rather than conventional coagulation.

The true contribution of the added coagulants becomes evident when comparing removal efficiencies above this baseline. For $FeCl_3$ and $Al_2(SO_4)_3$, incremental improvements in residual turbidity, TSS, and COD (e.g., TSS removal increasing from 93.3% to 100% with 30 mg/L $FeCl_3$ in Table 4) indicate that the added metal ions play a refining role. At extreme alkaline conditions, these metals form anionic hydroxo complexes (e.g., $Fe(OH)_4^-$, $Al(OH)_4^-$) that can adsorb onto the positively charged surfaces of freshly precipitated Ca^{2+}/Mg^{2+} particles, acting as bridging agents to enhance floc density and settling [7]. This incremental benefit, while modest in percentage terms for parameters already achieving >99% removal, is critical for consistently meeting the most stringent discharge limits, particularly for TSS and residual turbidity. For *Moringa oleifera*, its cationic proteins are likely impaired at pH > 11, so its modest additional removal is probably due to organic matter being passively enmeshed within the sweeping flocs, explaining its narrow effective window and performance decline at higher doses [5,19]. In conclusion, the overall treatment efficiency results from a synergistic combination: NaOH-driven precipitation of hardness ions creates the primary sweeping flocs, while the added coagulants refine floc structure and enable the system to consistently achieve the most stringent discharge limits.

4.2. Insights from RSM Optimisation and Model Validity

The application of RSM with a Central Composite Design proved highly effective in modelling the complex, non-linear interactions between pH, coagulant dosage, and multiple response variables. The high R^2 values (>0.97 for turbidity, colour, and COD) and insignificant lack-of-FIT tests ($p > 0.05$) for the primary models confirm that the quadratic polynomial models adequately represent the system within the experimental domain. The successful external validation, with low prediction errors (e.g., average RMSE of 5.mg/L for COD), affirms the models' robustness and practical utility for predicting treatment outcomes under varied conditions.

The lower R^2 for TSS (0.89) is attributed to greater inherent variability in biological floc characteristics in the secondary effluent, which affects settleability more than turbidity or colour. TSS removal is particularly sensitive to floc density and settling dynamics, which can be influenced by variable organic content and particle size distribution in the trickling filter effluent. This variability is not fully captured by the quadratic model, resulting in slightly lower predictive accuracy compared to the other parameters.

The multi-response optimisation using desirability functions provided a pragmatic solution to the common engineering challenge of balancing competing treatment goals [16]. For instance, maximising turbidity removal often required a higher pH, which had a less pronounced effect on COD reduction. The desirability approach allowed for the identification of a compromise optimum that achieved high performance across all four key water quality indicators, demonstrating a methodology superior to single parameter optimisation [26,27].

4.3. Regulatory Compliance and Economic Viability

The core impetus for this study was the longstanding non-compliance of the Palapye PETRO system. The proposed placement of the coagulation unit between the trickling filters (secondary treatment) and humus tanks confirms its role as a tertiary polishing stage, targeting residual pollutants after biological oxidation. When evaluated against Botswana's Effluent Standards for Wastewater Discharge, Botswana Department of Water Affairs (2012) [4], the optimised coagulation process presents a viable solution for compliance. The relevant standards for discharge into a dam (Lotsane) typically include limits for TSS, COD, and turbidity. Under the optimal conditions identified for $FeCl_3 \cdot 6H_2O$ (30 mg/L, pH 12), the treated effluent quality was assessed for compliance, as summarised in Table 10.

Table 10. Compliance assessment of optimised coagulation effluent against national standards.

Parameter	Botswana Standard (Typical Limit)	Optimised Effluent Value ($FeCl_3$)	Compliance Status
TSS	$\leq$30 mg/L	1 mg/L	Fully Compliant
COD	$\leq$75 mg/L	55 mg/L	Fully Compliant
Turbidity	$\leq$10 NTU	0.07 NTU	Fully Compliant

Source for Standards: Botswana Department of Water Affairs (2012) [4].

This analysis confirms that integrating a coagulation-flocculation unit between the trickling filters and humus tanks can bring the plant into full regulatory compliance for the critical parameters of TSS, COD, and turbidity. The economic analysis (Section 3.5, Table 9) indicates manageable operational costs, with $FeCl_3$ at approximately USD 0.089/m^3. While *Moringa oleifera* offers a lower chemical cost ($0.034/$m^3$), its sensitivity to overdosing and lower COD removal efficiency necessitate more sophisticated dosing control, potentially increasing operational complexity and cost [26,28]. Therefore, for guaranteed, consistent compliance, $FeCl_3$ is recommended despite its slightly higher chemical cost. The capital investment for dosing equipment ($15,000–$20,000) is modest compared to the cost of major plant upgrades or non-compliance penalties.

4.4. Limitations and Recommendations for Future Work

This study was conducted at the laboratory (Jartest) scale, which is an essential first step but has inherent limitations. Scaling up to full plant operation may introduce variables such as fluctuating inflow characteristics, imperfect mixing, and differences in settling dynamics [25,28]. Therefore, a pilot-scale trial is strongly recommended as the next step before full implementation.

Furthermore, the study focused on physicochemical parameters (turbidity, colour, COD, TSS). Future work should investigate the impact of this coagulation stage on downstream processes, particularly disinfection (e.g., chlorine demand may change) and the fate of nutrients (Nitrates, Phosphates). The effect of sludge production from the added coagulants on the existing sludge handling processes at the plant also requires evaluation.

Lastly, while *Moringa oleifera* showed limitations in this secondary effluent context, its potential as a sustainable, low-cost pre-coagulant or in hybrid treatment schemes (e.g., combined with a reduced dose of $FeCl_3$) warrants further investigation [26] to harness its benefits while mitigating its drawbacks.

4.5. Residual Metals: A Priority for Future Work

An important consideration for full-scale implementation is the residual concentration of coagulant-derived metals (Al^{3+}, Fe^{3+}) in the final effluent. At optimal pH (12–12.6),

aluminium shifts to soluble aluminate ($Al(OH)_4^-$), potentially increasing residual Al [15]. Iron, while less soluble across a broad pH range, also requires verification [7].

Notably, in magnesium-bearing waters such as secondary effluent, Al^{3+} may precipitate as hydrotalcite (Mg^{2+}-Al^{3+} layered double hydroxide) at high pH, effectively scavenging Al^{3+} from solution [7,29]. This mechanism could mitigate residual Al^{3+} concerns at Palapye, but direct experimental confirmation is lacking. Therefore, future work must quantify residual Al^{3+} and Fe^{3+} concentrations under optimal conditions and compare results against Botswana's discharge standards, Botswana Department of Water Affairs (2012) [4]. If national standards lack Al^{3+}/Fe^{3+} limits, comparison with international guidelines (WHO, USEPA) or ecotoxicological benchmarks [2,6] is recommended. Long-term monitoring of sediment accumulation in the Lotsane dam would also assess potential metal enrichment over time. Addressing this gap ensures comprehensive environmental protection.

5. Conclusions

This study successfully demonstrates that coagulation-flocculation can be effectively integrated as an enhancement to the secondary treatment stage to remediate the longstanding non-compliance of the Palapye PETRO wastewater treatment system. The systematic application of Response Surface Methodology (RSM) with Central Composite Design (CCD) enabled the efficient optimisation of multiple, interacting process variables—pH and coagulant dosage—for three distinct coagulants.

The key outcomes are as follows:

1. Ferric chloride ($FeCl_3 \cdot 6H_2O$) emerged as the most effective coagulant, achieving the highest and most consistent multi-parameter removal, particularly for turbidity and TSS, under alkaline conditions (pH 12, 30 mg/L). Aluminium sulphate provided robust performance, while *Moringa oleifera*, though cost-effective at low doses, exhibited a narrow optimal dosage window beyond which performance deteriorated due to restabilisation.
2. Statistically significant quadratic models were developed with high predictive accuracy ($R^2 > 0.97$ for key parameters). External validation with 3 independent experimental runs confirmed the models' reliability for forecasting treatment outcomes within the defined operational space.
3. The optimised $FeCl_3 \cdot 6H_2O$ process produced effluent meeting Botswana's discharge standards for TSS ($\leq$30 mg/L), COD ($\leq$75 mg/L), and turbidity ($\leq$10 NTU), directly addressing the plant's core compliance failure. Future work should quantify residual aluminium and iron concentrations to confirm environmental safety and regulatory compliance for coagulant-derived metals, particularly given the high-pH operating conditions [4,7].
4. The research provides a clear, data-driven pathway for implementation. Coagulant dosing can be integrated into existing infrastructure between the trickling filters and humus tanks with modest capital investment (USD 15,000–20,000). A detailed economic analysis (Table 9) indicates operational costs are manageable (USD 0.034–0.089/m^3), with $FeCl_3$ representing the optimal balance of performance and reliability for ensuring consistent compliance.

Therefore, this work not only presents a viable technical solution for the Palapye facility but also offers a replicable methodology for optimising and enhancing wastewater treatment systems in similar contexts globally.

Supplementary Materials: The following supporting information can be downloaded at: https://www.mdpi.com/article/10.3390/separations13050141/s1. Table S1: Full central composite design

matrix with experimental results for turbidity, colour, COD, and TSS removal. Table S2: Complete ANOVA results for the turbidity response surface quadratic model. Table S3: Complete ANOVA results for the colour response surface quadratic model. Table S4: Complete ANOVA results for the COD response surface quadratic model. Table S5: Complete ANOVA results for the TSS response surface quadratic model and Table S6: FIT Statistics Summary.

Author Contributions: Conceptualization: N.M.B. and P.T.O.; Methodology: N.M.B.; Software: N.M.B.; Validation: N.M.B. and P.T.O.; Formal analysis: N.M.B.; Investigation: N.M.B.; Resources: P.T.O.; Data curation: N.M.B.; Writing—original draft: N.M.B.; Writing—review and editing: P.T.O.; Visualisation: N.M.B.; Supervision: P.T.O.; Project administration: P.T.O. All authors have read and agreed to the published version of the manuscript.

Funding: This research received no external funding.

Data Availability Statement: The original contributions presented in this study are included in the article. Further inquiries can be directed to the corresponding author.

Acknowledgments: The authors acknowledge the support from the University of Botswana Department of Civil Engineering and the Mmamashia Water Utilities Corporation laboratory staff.

Conflicts of Interest: Nkgopolang Mathews Boima was employed by the company Water Utilities Corporation. The remaining author declares that the research was conducted in the absence of any commercial or financial relationships that could be construed as a potential conflict of interest.

Abbreviations

The following abbreviations are used in this manuscript:

$Al_2(SO_4)_3 \cdot 18H_2O$	Aluminium sulphate octadecahydrate
ANOVA	Analysis of Variance
AP	Anaerobic Pond
AS	Activated Sludge
BOD	Biological Oxygen Demand
CCD	Central Composite Design
CI	Confidence Interval
COD	Chemical Oxygen Demand
DOE	Design of Experiment
$FeCl_3 \cdot 6H_2O$	Ferric chloride hexahydrate
FP	Facultative Pond
HT	Humus Tank
MP	Maturation Pond
MRS	Multi-Response Surface
NTU	Nephelometric Turbidity Units
OFAT	One-Factor-at-a-Time
PETRO	Pond Enhanced Treatment and Operation
PWWTP	Palapye Wastewater Treatment Plant
RMSE	Root Mean Square Error
RSM	Response Surface Methodology
SS	Suspended Solids
TF	Trickling Filter
TSS	Total Suspended Solids
USEPA	United States Environmental Protection Agency
WHO	World Health Organisation
WSP	Waste Stabilisation Pond

References

1. Metcalf & Eddy, Inc. *Wastewater Engineering: Treatment and Resource Recovery*, 5th ed.; McGraw-Hill: New York, NY, USA, 2014.

2. Mara, D.D. *Domestic Wastewater Treatment in Developing Countries*; Earthscan: London, UK, 2004.
3. Gopolang, O.P.; Letshwenyo, M.W. Performance evaluation of waste stabilisation ponds. *J. Water Resour. Prot.* **2018**, *10*, 1129–1147. [CrossRef]
4. Botswana Department of Water Affairs. *Effluent Standards for Wastewater Discharge*; Government Printer: Gaborone, Botswana, 2012.
5. El Ouadrhiri, F.; Saleh, E.A.M.; Lahkimi, A. From mineral salts to smart hybrids: Coagulation–flocculation at the nexus of water, energy, and resources—A critical review. *Processes* **2025**, *13*, 3405. [CrossRef]
6. Verma, A.K.; Dash, R.R.; Bhunia, P. A review on chemical coagulation/flocculation technologies for removal of colour from textile wastewater. *J. Environ. Manag.* **2012**, *93*, 154–168. [CrossRef]
7. Irfan, M.; Butt, T.; Imtiaz, N.; Abbas, N.; Khan, R.A.; Shafique, A. Treatment of pulp and paper mill effluent using coagulation–flocculation process. *J. Environ. Chem. Eng.* **2017**, *5*, 4026–4034.
8. Maurya, S.; Daverey, A. Evaluation of plant-based natural coagulants for municipal wastewater treatment. *3 Biotech* **2018**, *8*, 77. [CrossRef]
9. Ndabigengesere, A.; Narasiah, K.S.; Talbot, B.G. Active agents and mechanism of coagulation of turbid waters using *Moringa oleifera*. *Water Res.* **1995**, *29*, 703–710. [CrossRef]
10. APHA; AWWA; WEF. *Standard Methods for the Examination of Water and Wastewater*, 23rd ed.; American Public Health Association: Washington, DC, USA, 2017.
11. García Ávila, F.F.; Mayancela Santander, E.F.; Alvarado Pacheco, M.B.; Valdiviezo Gonzáles, L.; Cadme Galabay, M.; Zhindón Arévalo, C.; Reynoso Quispe, P. Comparative analysis of coagulants for selective removal of iron and aluminium from galvanic wastewater. *Ain Shams Eng. J.* **2025**, *16*, 103393. [CrossRef]
12. Sánchez-Martín, J.; Ghebremichael, K.; Beltrán-Heredia, J. Comparison of single-step and two-step purified coagulants from Moringa oleifera seed for turbidity and DOC removal. *Bioresour. Technol.* **2010**, *101*, 6259–6261. [CrossRef]
13. Desta, W.M.; Bote, M.E. Wastewater treatment using a natural coagulant (*Moringa oleifera* seeds): Optimization through response surface methodology. *Heliyon* **2021**, *7*, e08451. [CrossRef]
14. Machlor, A.; Sreekrishnan, T.R.; Tyagi, R.D. Optimization of coagulation-flocculation process using response surface methodology: A critical review. *Environ. Technol. Rev.* **2022**, *11*, 45–67.
15. Montgomery, D.C. *Design and Analysis of Experiments*, 10th ed.; John Wiley & Sons: Hoboken, NJ, USA, 2019.
16. Comet Manesa, K.; Dyosi, Z. Review on *Moringa oleifera*, a green adsorbent for contaminants removal: Characterization, prediction, modelling and optimization using Response Surface Methodology (RSM) and Artificial Neural Network (ANN). *J. Environ. Sci. Health Part A* **2023**, *58*, 1014–1027. [CrossRef] [PubMed]
17. Derringer, G.; Suich, R. Simultaneous optimization of several response variables. *J. Qual. Technol.* **1980**, *12*, 214–219. [CrossRef]
18. Gregory, J. *Particles in Water: Properties and Processes*; IWA Publishing: London, UK, 2006.
19. Chira, M.N.; Amariei, S. Study on the Effect of Heavy Metal Contamination of Milk on the Coagulation Process. *Foods* **2026**, *15*, 1498. [CrossRef]
20. Baghvand, A.; Daryabeigi Zand, A.; Mehrdadi, N.; Karbassi, A. Optimizing coagulation process for low to high turbidity waters using aluminum and iron salts. *Am. J. Environ. Sci.* **2010**, *6*, 442–448. [CrossRef]
21. Pérez, A.G.; García, M.C.; Sánchez, L. pH-induced coagulation mechanisms in wastewater treatment. *J. Water Process Eng.* **2017**, *19*, 120–128.
22. Ebba, M.; Asaithambi, P.; Alemayehu, E. Investigation on operating parameters and cost using an electrocoagulation process for wastewater treatment. *Appl. Water Sci.* **2021**, *11*, 175. [CrossRef]
23. Shaylinda, M.Z.N.; Aziz, H.A.; Adlan, M.N.; Yusoff, M.S.; Bashir, M.J.K. Application of response surface methodology for optimization of ammoniacal nitrogen removal. *Desalin. Water Treat.* **2018**, *128*, 334–343.
24. Wang, P.; Chen, Y.-Z.; Wang, Y.; Yuan, S.-J.; Yu, H.-Q. Optimization of the coagulation-flocculation process for pulp mill wastewater treatment using a combination of uniform design and response surface methodology. *Water Res.* **2011**, *45*, 5633–5640. [CrossRef]
25. Tetteh, E.K.; Rathilal, S.; Chetty, M. Application of Moringa oleifera in wastewater treatment: A review of mechanisms and performance. *Environ. Sci. Pollut. Res.* **2022**, *29*, 43157–43179.
26. Pritchard, M.; Mkandawire, T.; O'Neill, J.G. Sustainable water treatment using Moringa oleifera: A 15-year perspective. *Phys. Chem. Earth* **2021**, *122*, 102992.
27. Koul, B.; Bhat, N.; Abubakar, M.; Mishra, M.; Arukha, A.P.; Yadav, D. Application of Natural Coagulants in Water Treatment: A Sustainable Alternative to Chemicals. *Water* **2022**, *14*, 3751. [CrossRef]

28. Camacho, F.P.; Sousa, V.S.; Bergamasco, R.; Teixeira, M.R. The use of *Moringa oleifera* as a natural coagulant in surface water treatment. *Chem. Eng. J.* **2017**, *313*, 226–237. [CrossRef]
29. Liu, Y.; Wang, J.; Zhang, X.; Li, H. Layered double hydroxides for water treatment: Recent advances and future perspectives. *Chem. Eng. J.* **2023**, *458*, 141489.